Stable Immobilization of DNA to Silica Surfaces by Sequential Michael-Addition Reactions Developed with Insights from Confocal-Raman Microscopy

Grant J. Myres and Joel M. Harris*

Department of Chemistry, University of Utah, 315 South 1400 East

Salt Lake City, UT 84112-0850 USA

Abstract

The immobilization of DNA to surfaces is required for numerous biosensing applications related to capture of target DNA sequences, proteins, or small-molecule analytes from solution. For these applications to be successful, the chemistry of DNA immobilization should be efficient, reproducible, and stable and should allow the immobilized DNA to adopt secondary structure required for association with its respective target molecule. To develop and characterize surface-immobilization chemistry to meet this challenge, it is invaluable to have a quantitative, surface-sensitive method that can report the interfacial chemistry at each step, while also being capable of determining the structure, stability, and activity of the tethered DNA product. In this work, we develop a method to immobilize DNA to silica, glass, or other oxide surfaces by carrying out the reactions in porous-silica particles. Due to the high specific surface area of porous silica, the local concentrations of surface-immobilized molecules within the particle are sufficiently high that the interfacial chemistry can be monitored at each step of process with confocal-Raman microscopy, providing a unique capability to assess the molecular composition, structure, yield, and surface-coverage of these reactions. We employ this methodology to investigate the steps for immobilizing thiolated-DNA to thiol-modified silica surfaces through sequential Michael-addition reactions with the cross-linker 1,4-phenylene-bismaleimide. A key advantage of employing a phenyl-bismaleimide over a comparable alkyl coupling reagent is the efficient conversion of the initial phenyl-thiosuccinimide to a more stable succinamic-acid thioether linkage. This transformation was confirmed by in situ Raman spectroscopy measurements, and the resulting succinamic-acid thioether product exhibited greater than 95% retention of surfaceimmobilized DNA after 12 days at room temperature in aqueous buffer. Confocal-Raman microscopy was also used to assess the conformational freedom of surface-immobilized DNA by comparing the structure of a 23-mer DNA hairpin sequence under duplex-forming and unfolding conditions. We find that the immobilized DNA hairpin can undergo reversible intramolecular duplex formation based on changes in frequencies and intensities of phosphate-backbone and base-specific vibrational modes that are informative of the hybridization state of DNA.

* Corresponding author: harrisi@chem.utah.edu

INTRODUCTION

The immobilization of DNA at solid-liquid interfaces underlies numerous biosensing technologies. In many applications, the selective binding interactions between surface immobilized DNA with solution phase complimentary oligonucleotides, small molecules, or proteins are detected and characterized. Studying non-covalent binding interactions has enabled the development of both fundamental research and applied sensing applications related to detecting analytes in complex samples, ¹⁻⁴ gene profiling for disease diagnostics, ⁵⁻⁷ and understanding the reversible interactions of DNA with small-molecules ⁸⁻¹⁴ and proteins ^{8,15-17} that regulate gene expression. For these applications of surface-immobilized DNA, it is crucial that the surface-conjugation chemistry be efficient, reproducible, and stable. Additionally, the immobilized DNA must be able to adopt the appropriate secondary structure that enables the specific association interactions with a target molecule.

In this work, we employ confocal-Raman microscopy to guide the development of an efficient and stable cross-linking approach to immobilize DNA to silica surfaces. In previous research from this lab, we immobilized amine-conjugated DNA to epoxide-modified glass surfaces; however, the inefficiency of amine-epoxide coupling required high solution concentrations of aminated-DNA reacted at high temperatures to carry out the immobilization. The resulting surface coverages of probe DNA were modest ($\leq 5 \times 10^{10}$ molecules/cm²) but adequate for imaging of hybridization events of individual fluorescently-labeled DNA molecules. In order to immobilize DNA at much greater densities, a more efficient means of surface-immobilization of DNA is needed.

Michael-addition reactions between thiol and maleimide functional groups (Figure 1) are an attractive alternative to meet this need; the reaction proceeds rapidly^{21,22} under mild conditions without the need of a catalyst, embodying many of the attractive attributes of a 'click' chemistry.^{23,24} Despite these attributes, thiol-maleimide Michael-addition coupling for surface conjugation comes with a caveat: the thiosuccinimide product formed by the Michael addition is unstable and is susceptible to a retro-Michael addition resulting in the undesired cleavage of the sulfur-succinimide bond (Figure 1).^{22,25-27} An alternative fate of the thiosuccinimide product is a ring-opening hydrolysis, which yields a more robust and stable succinamic-acid thioether linkage.^{28,29} The relative rates of these pathways depend on the electronic properties of the functional group adjacent to the succinimide. For bioconjugate chemistry applications, alkyl-maleimide reagents have been conventionally used,^{26,30,31} where the adjacent alkyl group has a weak electron donating effect on the neighboring thiosuccinimide making them resilient to hydrolysis (Figure 1). Molecules conjugated by alkyl-maleimides typically degrade by retro-Michael addition, which over time results in undesirable bond cleavage and

deconjugation. This issue was observed in previous work from our lab,³² where alkylmaleimide-modified DNA immobilized to thiolated silica was found to dissociate from the surface upon long-term storage in buffer, an observation that provided motivation for the present work.

Issues related to the poor stability of the thiosuccinimide linkage have been circumvented bv phenvluse maleimides in place of alkyl-maleimide coupling reagents. Phenyl-maleimides react with thiols to form thiosuccinimides that readily hydrolyze in aqueous buffer to form a more robust and stable succinamicacid thioether conjugate linkage (Figure 1).^{28,29} Efficient hydrolysis has been attributed to the adjacent phenylgroup delocalizing the nitrogen lone-pair electrons, making the neighboring

Figure 1. Michael-addition reaction between a thiol and maleimide forming a thiosuccinimide (top), which undergo the following reactions. Thiosuccinimides can react via a retro-Michael addition reaction resulting in bond cleavage (middle). Alkyl-thiosuccinimides are stable to base-catalyzed hydrolysis, while phenyl-thiosuccinimide can undergo ring-opening hydrolysis forming a stable succinamic acid thioether product (bottom).

carbonyl carbons more electrophilic and susceptible to a nucleophilic attack by water. Although phenyl-maleimides have been successfully used for the conjugation of small-molecules to cysteineresidues in proteins, (phenyl-maleimide)-thiol chemistry has yet to be applied to enhance the stability of biomolecule coupling to solid surfaces. This is likely due to the poor hydrolytic stability of phenyl-maleimide reagents, where the half-life of the intact imide ring in aqueous solution can be as short as minutes to a few hours depending on pH. (28,29,34)

In this work, we develop a protocol using a bifunctional reagent, N,N'-1,4-phenylene-bismaleimide, to cross-link thiol-functionalized DNA to thiol-modified porous silica surfaces. The immobilization approach exploits the reactivity of thiols and maleimides,²⁹ while avoiding issues related to poor hydrolytic stability^{28,29,34} of the phenyl-maleimide-modified DNA conjugate by immediately reacting the DNA-maleimide with the thiolated-silica surface. Because the chemistry is carried out on a high-surface-area porous silica support, there is a sufficient population of molecules

on the interior surfaces of the particle to allow confocal-Raman microscopy to characterize the interfacial composition *through each step of surface-immobilization and modification*. Raman scattering spectra are quantitative and were used to determine the surface coverage of the immobilized DNA. They also reveal that the resulting DNA surface-conjugate undergoes hydrolytic conversion of the thiosuccinimide to a more stable succinamic-acid thioether linkage. The conformational freedom of the surface-tethered DNA was tested with confocal-Raman microscopy to assess the ionic strength-dependent intramolecular hybridization of an immobilized DNA hairpin.

EXPERIMENTAL SECTION

Reagents and materials. Spherical chromatographic silica particles was purchased from YMC America (Devens, MA) with an average particle diameter of 5-um, a pore diameter of 31 nm, and a specific surface area of 117 m²/g, as specified by the manufacture. The 2,2-dimethoxy-a-thia-2-silacyclopentane used for surface conjugation of the silica with thiol groups was purchased from Gelest (Morrisville, PA). Samples of DNA conjugated with disulfide groups prepared by solid-phase synthesis by the University of Utah HSC Care DNA Synthesis Facility, using the 5'-hexyl disulfide-phosphoramidite modifier (C6 SS) from Glen Research (Maravai LifeSciences, San Diego, CA). The principal DNA sequence used in these experiments was a 23-base hairpin sequence: (C6 SS)-5'-CCC CGA ATT CGT CTC CGA ATT CG-3'. A simpler, exclusively-GT 18-base sequence that produces less congested Raman spectra was used in testing surface-conjugation stability: (C6 SS)-5'-TTT GGT TGG TGT GGT TGG-3'.

Water used in experiments was filtered with a Barnstead GenPure UV water purification system (ThermoFisher, Waltham, MA) and had a minimum resistivity of $18.0~\text{M}\Omega\cdot\text{cm}$. N-phenylmaleimide, dichloromethane (DCM), ethyl-maleimide, 1,11-bismaleimido-triethylene glycol, sodium chloride, dithiothreitol, sodium azide, and tris(2-carboxyethyl)phosphine hydrochloride (TCEP) were purchased from Sigma-Aldrich (St. Louis, MO); N,N'-1,4-phenylene-bismaleimide and triethylamine from TCI (Tokyo), dimethylformamide (DMF), hydrogen peroxide, sodium hydroxide, hydrochloric acid, and sodium phosphate dibasic heptahydrate (Na₂HPO₄ 7H₂O) were purchased from ThermoFischer Scientific. 2-amino-2-(hydroxymethyl)propane-1,3-diol was purchased from Goldbio (St. Louis, MO).

Thiol functionalization of silica. A 20-mg sample of silica particles was washed with a solution of acid piranha (60:40 concentrated sulfuric acid/30% hydrogen peroxide; caution: corrosive, strong oxidizer, and can react explosively with organics) to remove physisorbed carbon compounds

from the silica surface. Following the piranha acid wash, the sample of particles was rinsed with deionized water twice, followed by a wash in ethanol twice and finally a wash in anhydrous DCM five-times. Particle samples were suspended in 1 mL of DCM and 50 uL of 2,2-dimethoxy-1-thia-2-silcyclopentane was finally added to the particle dispersion and allowed to react on a shake-plate for 1 hour. Following the reaction, excess silane reagent was quenched with ethanol and the sample was washed in ethanol twice followed by a wash in deionized water three-times to remove ethanol. Particles were stored in deionized water at 2°C; surface immobilized thiol-groups were stable for months as verified by Raman spectroscopy (see below).

Reduction of disulfide-DNA to thiol-DNA. Samples of 5'-disulfide-conjugated DNA was prepared by the University of Utah DNA and Peptide Core Facility. To reduce the disulfide for maleimide conjugation, ~500 nmols of lyophilized disulfide-DNA was rehydrated in 200 μL of 10 mM pH 8 tris buffer prepared with 50 mM DTT, 1 mM EDTA, and 2% triethylamine. Following a 20-minute reaction, a purification by precipitation of the DNA by addition of 30 μL of 3-M sodium acetate pH 5.2 followed by addition of 575 μL of ethanol at -20 °C. Following the addition of ethanol, the sample appeared cloudy due to precipitate formation; the sample was then centrifuged (2 minutes, 14,000 rpm) and the DTT containing supernatant was removed. The sample was washed in ethanol 5-times to remove excess DTT. In the final ethanol wash, the excess ethanol was removed by vacuum for 20-minutes. The sample was then rehydrated in deionized water and stored at 2 °C.

Coupling thiol-DNA to the thiolated silica surface. For coupling the thiol-DNA to the thiolsilica surface, reaction of thiol-DNA to 1,4-phenylene-bismaleimide with a >10-fold molar excess of 1,4-phenylene-bismaleimide in 50/50 (v/v) DMF/Tris buffer pH 7.4 with 200-mM NaCl and 500-uM TCEP (12-uL final volume) was carried out for 10 minutes. Following the reaction, the maleimide-conjugated DNA product was separated by precipitation from the excess bismaleimide by addition of 30 μL of ethanol (-20°C). Following centrifugation (2 minutes, 14,000 rpm), the DNA pellet was washed in ethanol twice followed by 2 washes with DMF and a final wash with ethanol to remove traces of bismaleimide. The ethanol was then removed by evaporation under vacuum for ~10 minutes. Following this purification step, the maleimide-conjugated DNA was rehydrated with aqueous 400-mM NaCl, immediately diluted with an equal volume of DMF, and allowed to react with thiol-functionalized silica particles for 12-hours.

Confocal-Raman microscopy. Confocal-Raman microscopy has been described in detail elsewhere.³⁵ Briefly, a 647.1 nm excitation beam from a Kr⁺ laser (Innova 90, Coherent Int., Santa Clara, CA) was propagated though a bandpass filter and passed through a x4 beam expander (50-25-

4x-647, Special Optics Inc., Wharton, NJ) and reflected off a dichroic beam splitter, and directed into a 1.4-NA, 100x oil-immersion objective (CFL PLAN APO, Nikon Inc., El Segundo, CA), producing a focus with a ~600 nm diameter beam waist. Scattered light from the confocal probe volume was collected by the same objective, transmitted though the dichroic beam splitter, passed thought a long pass filter, and finally focused though the 50-μm slit of a 500-mm focal-length spectrograph (Bruker 500IS) with a 300-line/mm diffraction grating blazed at 750 nm. Light diffracted off the grating was projected onto a charged coupled device (iDus 401A, Andor USA, South Windsor, CT).

Well cells for confocal-Raman microscopy were constructed by adhering a ~12 mm length of 10-mm i.d., 13-mm o.d. Pyrex glass tubing to a No. 1 glass coverslip using Devcon 5 min epoxy (ITW Devcon, Danvers, MA). To collect spectra, the beam was focused at the solution/coverslip interface and adjusted upward in the z-dimension until particles were in the field of view. The stage was then adjusted in the x and y dimensions until the focus and confocal probe volume was centered in a single porous silica particle. Each spectrum reported represented 2-minute integrations collected from 6 different individual particles. All the collected spectra were truncated to the frequency region of interest and baseline corrected with a rolling-circle algorithm.³⁶ Data analysis was carried out in Matlab (Mathworks, Natick, MA) using custom scripts. Depending on the chemistry being investigated, spectra were normalized to scattering from either the 1780 cm⁻¹ succinimide stretch or the 3430 cm⁻¹ OH stretch of water.

RESULTS AND DISCUSSION

Immobilization and reactivity of surface-immobilized thiols. To immobilize thiol groups to mesoporous silica interfaces, a cyclic-thiasilane reagent was used.³⁷ The advantage of this reagent over traditionally-used trialkoxysilane reagents is the formation of the siloxane bond progresses under anhydrous conditions and is not susceptible to cross-linking^{37,38} that can result in dimerization or polymerization during the surface-functionalization step. At each step of the immobilization chemistry, confocal-Raman microscopy was used to characterize the interfacial chemical composition of mesoporous silica particles.³⁹ Raman spectra of bare silica (Figure 2) shows silica framework vibrational modes (700-1000 cm⁻¹) and a water bending mode (1640 cm⁻¹). Following the reaction of bare silica with 2,2-dimethoxy-1-thia-2-silacyclopentane (details in Experimental Section), the addition of both C-H and C-C modes (1100 – 1500 cm⁻¹) and the distinctive thiol S-H stretching mode (2580 cm⁻¹) is clear (Figure 2).

To assess whether the surfaceimmobilized thiol is reactive towards maleimide functional groups, thiolfunctionalized silica particles were reacted with 1-mM N-phenylmaleimide in 50/50 (v/v) DMF/pH 7.4 PBS for 1 hour and washed in PBS buffer to remove excess maleimide reagent and DMF. A spectrum of particles reacted with N-phenylmaleimide (Figure 2) shows nearly complete loss of the thiolstretch accompanied with the addition of phenyl ring breathing and C=C stretching modes (1003 and 1607 cm⁻¹) and the addition of a succinimide stretch (1780 cm⁻¹). Raman spectra show both

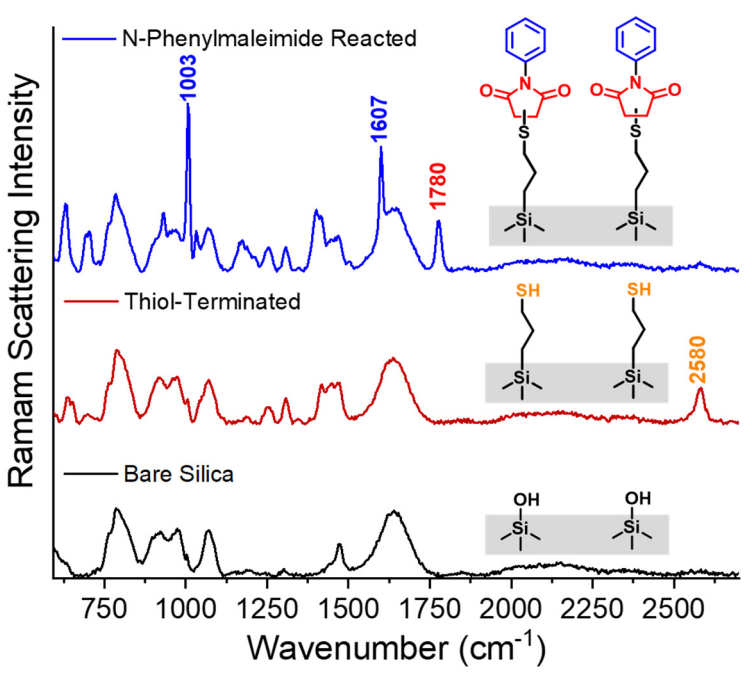


Figure 2. Thiol-immobilization at mesoporous silica surfaces and reaction with aryl-maleimide. Raman spectra of bare silica (bottom, black), after thiol immobilization (middle, red), and after reaction with N-phenylmaleimide (top, blue). Frequency labels of the functional group vibrations are color coded.

immobilization of the thiol and complete conversion of the immobilized thiol to a thiosuccinimide product following reaction with N-phenylmaleimide.

Preparation of maleimide-DNA for immobilization to thiol-functionalized silica. To conjugate thiol functionalized DNA to thiol-presenting silica surfaces, a cross-linking protocol was developed by performing sequential Michael addition reactions with a bismaleimide reagent (Scheme S1, Supporting Information). First, disulfide-modified DNA was reduced with DTT and isolated by precipitation from ethanol and centrifugation (see Experimental Section). The thiol-functionalized DNA was then reacted with a >10-molar excess of 1,4-phenylene-bismaleimide in 50/50 (v/v) DMF/Tris buffer for 10 minutes. Following the reaction, the maleimide-conjugated DNA was separated from excess unreacted bismaleimide by precipitation through the addition of 2.5 volume equivalents of ethanol at -20 °C. Following centrifugation, the DNA pellet was washed in ethanol twice, followed by 2 washes with DMF, and 2 final washes with ethanol to remove traces of bismaleimide; ethanol was then removed by evaporation under vacuum. As a check on the product and efficiency of the reaction, a sample of the DNA pellet was dissolved in deionized water, desalted, and analyzed by electrospray-ionization time-of-flight mass spectrometry. The mass spectrometry

results confirm the formation of the monomeric maleimide-conjugated DNA product, with no residual thiol-functionalized DNA and minimal (~1.5%) dimer DNA product (see Supporting Information).

For immobilization of the DNA to the porous silica particle surface, maleimideconjugated DNA (preparation and isolation described above) was dissolved in aqueous 400-mM NaCl and immediately diluted with an equal volume of DMF and allowed to with thiol-functionalized silica react particles for 12 hours. Following the reaction of the maleimide-DNA with thiolfunctionalized silica, the particles were washed by dilution and centrifugation in PBS buffer and characterized with confocal-Raman microscopy.

Comparing the spectra of thiolfunctionalized silica before and after the reaction with maleimide-conjugated DNA reveals immobilization of DNA by

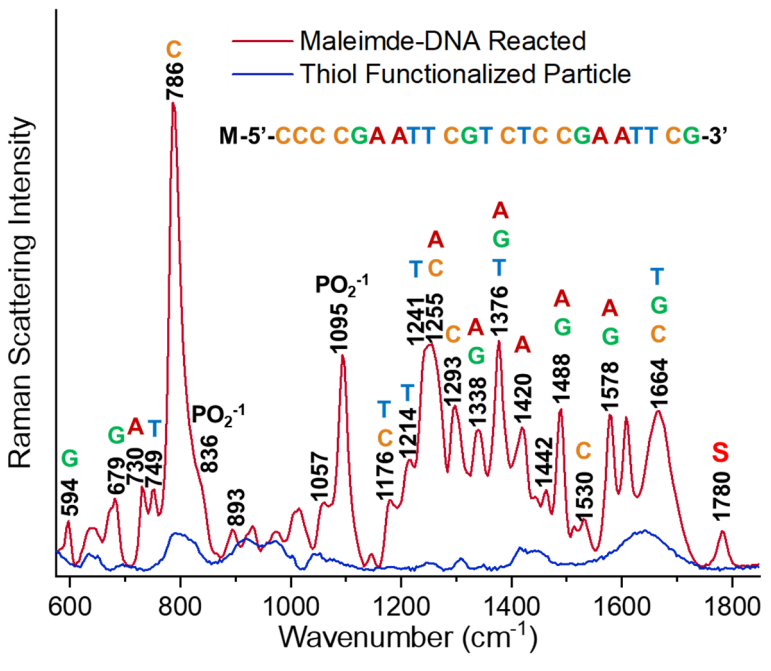


Figure 3. Surface-immobilization of DNA with 1,4-phenylenedimaleimde. Raman spectra of thiol-functionalized silica (bottom, blue) and thiolated silica reacted with maleimide-conjugated DNA (top, red). C = cytosine, C = guanine, C = guanine, C = cytosine, C = guanine, C = cytosine, C = guanine, and C = cytosine, and $C = \text{$

appearance of scattering from vibrational modes of DNA, which are identified in Figure 3. Additionally, observation of the thiosuccinimide stretch (1780 cm⁻¹) verifies that surface immobilization of DNA proceeds by the phenyl-bismaleimide cross-linking reagent forming succinimide bonds to the thiol-DNA and the thiolated-silica surface. The resulting surface density of the immobilized DNA was quantified by comparison of its thiosuccinimide Raman scattering intensity at 1780 cm⁻¹ to the scattering from an immobilized N-phenylmaleimide standard, the surface coverage of which was calibrated by elemental carbon analysis (Supporting Information). The immobilized DNA surface density, thus determined, was $2.8 \pm 0.6 \times 10^{13} \, \text{cm}^{-2}$, or a root-mean-square distance between immobilized DNA molecules of $1.9 \pm 0.2 \, \text{m}$. This surface density of DNA is comparable to a close-packed array of double-stranded B-form DNA having a helix diameter of ~2.0 nm. Compared to amine-epoxide coupling chemistry, the maximum achievable densities of DNA in the current example is more than 1000-times greater.

Surface stability of DNA immobilized with phenyl-bismaleimide coupling. Application of phenyl-maleimides for bioconjugate chemistry has long been limited and even avoided^{26,28} because of their rapid hydrolysis to maleamic acid especially under aqueous solution conditions.^{28,29} In the current work, we have developed surface immobilization of thiol-DNA with a phenylene-bismaleimide cross linking reagent that overcomes the hydrolytic stability of the phenyl-maleimide conjugated DNA intermediate by carrying out the surface immobilization step immediately following the initial conjugation in a partially organic solvent system. These reactions produce DNA immobilized to a thiolated silica surface through a pair of phenyl-thiosuccinimide linkages (Scheme S1).

Previous work has shown that phenyl-thiosuccinimides hydrolyze over time to form a succinamic acid thioether product, which has been shown to be stable (Figure 1). ^{26,33,41} This chemistry was tested on a guanine- and thymine-containing DNA sequence immobilized by the above protocol to thiolated porous silica. The sequence was chosen for its simple base composition that produces Raman spectra with better-resolved bands and allows more accurate quantitative analysis. To test the surface conjugation stability, a Raman spectrum of a sample of particles acquired immediately after their preparation was compared to the same sample following storage for 12-days at room temperature in pH 7.4 PBS buffer with 25 mM sodium azide. The two spectra are compared in Figure 3, where both spectra are normalized to scattering intensity at 3430 cm⁻¹ from the OH stretch of water that fills

the pores. Comparing the total DNA band intensity integrated from 600 to 1100 cm⁻¹ shows that 97± 5% of the original surface-immobilized DNA is retained after 12 days in buffer. The origin of this stability is also apparent in Figure 4, where the Raman spectra reveal changes in the surface-coupling chemistry over time. While the intensity of DNA bands in Figure 4 remains constant, the scattering intensity of the 1780 cm⁻¹ thiosuccinimide stretch decreases over time. This decrease in thiosuccinimide stretching intensity is accompanied by an increase in intensity of the C=C stretch (1612 cm⁻¹) and the appearance of scattering from

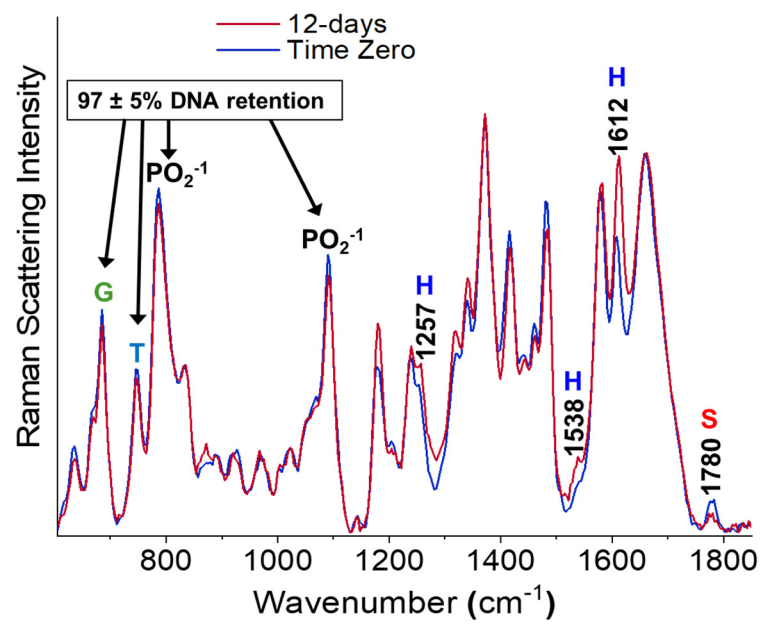


Figure 4. Conjugation stability of thiol-DNA immobilized by 1,4-phenylenedimaleimide over the course of 12-days. Time zero (blue), 12 days (red). G = guanine, T = thymine, $PO_2^{-1} = phosphate$, S = succinimide, H = hydrolysis product.

new bands at 1257, and 1538 cm⁻¹ consistent with amide III and amide II stretching modes that arise from the hydrolysis of the thiosuccinimide bonds and formation of a succinamic acid thioether product (Figure 1). These changes in structure are more apparent in time-dependent data acquired for hydrolysis of a simple immobilized phenyl-thiosuccinimide, prepared by reacting the thiol-functionalized silica with N-phenylmaleimide (see Supporting Information, Figure S3). Without interference from DNA scattering, the observed changes in band intensities and appearance of amide modes are clear and consistent with hydrolysis of the thiosuccinimide over time to form a more stable succinamic acid thioether product.

To determine how the stability of the phenyl-bismaleimide immobilized DNA compares to alkyl-bismaleimide coupling, we also immobilized thiol-DNA to the thiolated-silica surface using 1,11-bismaleimido-triethyleneglycol as cross-linker. DNA immobilized with the alkyl-bismaleimide was subjected to equivalent conditions as the DNA immobilized with the phenyl-bismaleimide described above. Over the same time (12-days) in PBS buffer, Raman scattering reveals that only $32 \pm 8\%$ of the original surface-immobilized DNA was retained (Supporting Information, Figure S4). Additionally, the loss of the DNA scattering intensity was correlated with the intensity decrease of the 1780 cm^{-1} succinimide mode responsible for surface coupling; suggesting dissociation is a result of the retro-Michael addition reaction.

These results collectively show that the phenyl group adjacent to the thiosuccinimide plays a key role in enhancing the surface stability of the DNA conjugate by increasing the efficiency of thiosuccinimide hydrolysis, resulting in the conversion of the thiosuccinimide to a more stable succinamic acid thioether. This result contrasts with the conventionally used alkyl-maleimides which form a thiosuccinimide product that was observed to dissociate over time due to its susceptibility to the retro-Michael addition.

Structure of porous-silica immobilized DNA. Stable immobilization of DNA strands on the interior surfaces of porous silica particles provides a local concentration of DNA within the particle interior that is sufficiently high (~30-mM) that confocal Raman microscopy can be used for label-free investigations of the structure and reactivity of the surface-immobilized DNA. We demonstrate this capability by examining the structure of the immobilized 23-mer DNA hairpin in response to changes in the ionic strength of the overlaying solution. DNA hairpins, like the 23-mer sequence immobilized above, are single-stranded DNA that can self-hybridize through intramolecular base-pairing and are commonly used as 'molecular beacons' in biosensing applications.^{42,43} When DNA hairpin molecular beacons are surface-immobilized for biosensing, surface-crowding effects^{44,45} can impact the stability

of folded versus unfolded states of the stem-loop or hairpin DNA structure. To respond as a molecular beacon, there must be sufficient freedom of motion for a DNA hairpin to unfold in response to the binding of an oligonucleotide target.

Our goal, therefore, was to test whether the 23-base DNA hairpin sequence that was immobilized at high densities on the porous silica surfaces can undergo a folded-to-unfolded transition that would be critical to a functioning biosensor. Raman spectroscopy is an informative method capable of discerning between single-stranded and duplex DNA conformations by shifts in the frequencies of scattering from both DNA bases and the phosphate-sugar backbone upon hybridization. While these previous Raman scattering studies were carried out with free-solution DNA samples, recent work from our lab showed that equivalent frequency shifts can be observed with immobilized ssDNA upon hybridization with complementary strands from solution. In the present case, we determine the conformational state of the immobilized DNA hairpin sequence, as its intramolecular hybridization responds to solution conditions, employing a reduction in ionic strength to destabilize the hybridized duplex structure. Because the backbone of DNA is highly charged with phosphate groups, complementary DNA strand regions must overcome significant electrostatic

Lowering the electrolyte concentration increases charge-charge repulsion through loss of counter-ion screening, thereby destabilizing the duplex^{50,51} and unfolding the compact hairpin structure.^{44,45}

repulsion in order to form a duplex.⁴⁹

The Raman spectra of the silicaimmobilized 23-mer DNA hairpin in phosphate-buffered saline (ionic strength 152 mM) and in deionized water are compared in Figure 5. While nucleobases have significant band overlap with one another in higher frequency regions of the Raman spectrum (1100 - 1700 cm⁻¹), the lower frequency region from 600 – 900 cm⁻¹

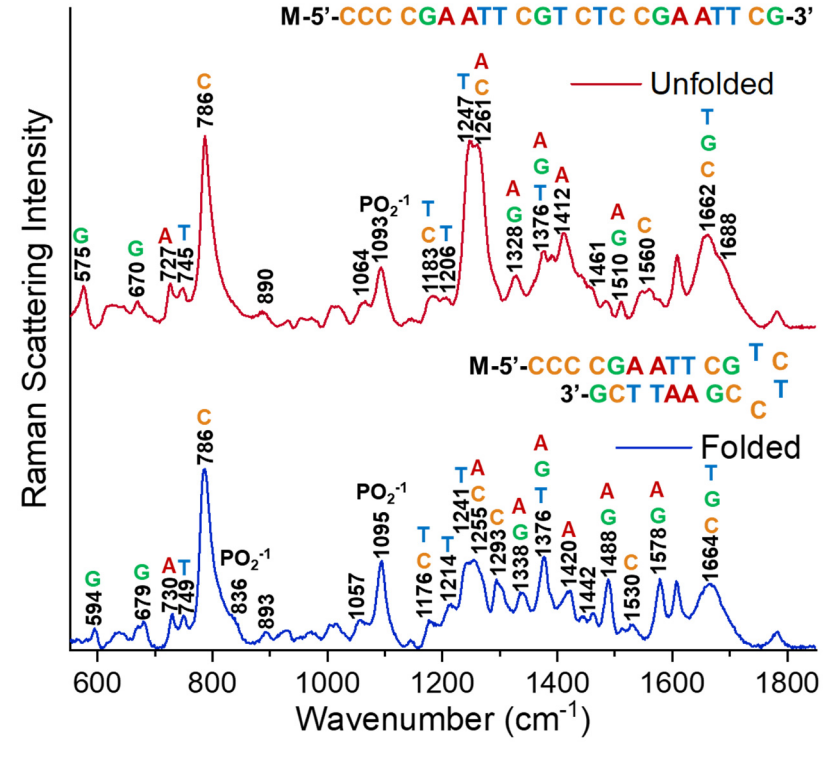


Figure 5. Comparison of surface immobilized 23-mer hairpin sequence of DNA in deionized water (top, red) and in saline buffer (bottom, blue). C = cytosine, C = guanine, C = cytosine, C = guanine, C = cytosine, C

contains several base-specific and phosphate-backbone vibrational modes unobscured by overlapping bands, which can be used to discern structural changes. Comparison of the surface immobilized hairpin sample in buffered saline versus deionized water reveals the guanine ring stretch shifts from 679 to 670 cm⁻¹, the adenine ring stretch shifts from 730 to 727 cm⁻¹ and the thymine ring stretch shifts from 749 to 745 cm⁻¹. These characteristic Raman scattering frequencies are consistent with duplex DNA transitioning to single-stranded DNA, as previously reported in DNA melting experiments. 46-48,52

Additionally, the 836 cm⁻¹ PO₂⁻¹ stretch, which is only present in B-Form duplex DNA,⁵² is absent in spectrum of the sample in deionized water, further evidence that the duplex region of the hairpin has unfolded. In addition to changes in band frequencies, the polarizabilities of several vibrational modes of DNA bases are reduced when they form duplexes due to electronic effects of base-stacking and base-pairing. 47,48 In agreement with this expectation, the intensities of the 1240 cm⁻¹ thymine mode and the 1668 cm⁻¹ carbonyl stretch of thymine, guanine, and cytosine are all substantially greater for the sample in deionized water where base-pairing is lost and the hairpin unfolds into a single-stranded DNA. Collectively, these results show that despite the high surface density at which the DNA is immobilized, the surface-immobilized DNA can freely transition from a compact DNA hairpin in high ionic-strength buffer to an unfolded random coil in deionized water. Despite the high surface coverage of the immobilized DNA, its conformational mobility may be due to the convex nature of the porous silica surfaces (see SEM image in Supporting Information); this convex surface structure likely derives from the synthesis of the xerogel material, which occurs by aggregation of silica sols to form porous particles.⁵³ As has been shown that the assembly of thiolterminated ssDNA on spherical gold colloids, particle diameters less than 30-nm allow higher surface coverage of DNA compared to flat surfaces due to the greater volume available away from the convex surface. 54,55 The solution volume away from a convex silica surface may provide the immobilized DNA hairpins the conformational freedom needed to unfold in low-ionic strength conditions. For applications where greater separation between immobilized DNA strands is needed (in protein-binding studies, for example), the DNA surface density can be lowered by either reducing the density of thiolsilane anchors on the silica surface or lowering the concentration and/or reaction time of maleimide-DNA in the surface-coupling step.

Summary and future perspective. With the guidance of Raman spectroscopy data at each step, a new approach to immobilize thiol-functionalized DNA to thiolated porous silica surfaces has been developed that utilizes a phenyl-bismaleimide cross-linking reagent. The method takes advantage of the reactivity of thiol and maleimide groups through sequential Michael-addition reactions. An

initial Michael addition reaction with thiol-DNA and phenyl-bismaleimide produces phenyl-maleimide conjugated DNA that can be isolated and then immediately reacted with thiol-functionalized silica to form the conjugate product. Hydrolysis of the phenyl-thiosuccinimides to the corresponding succinamic-acid thioethers produces more stable surface immobilization compared to alkyl-maleimide coupling whose thiosuccinimide bonds does not readily hydrolyze to the more stable product. The efficiency of phenyl-bismaleimide coupling can produce surface densities of the immobilized DNA that are close to the theoretical limit of a full monolayer. A unique aspect of this development was the use of Raman microscopy to monitor the surface composition, structure, and coverage of the immobilized DNA by carrying out the reactions on the interior surfaces of porous silica particles.

The DNA cross-linking methodology employing phenyl-bismaleimides for enhanced stability has the potential to be extended to the immobilization of other thiol-containing molecules at silica surfaces or the conjugation of thiolated oligonucleotides and other molecules to proteins or peptides through cysteine residues. The surface-conjugation chemistry is not limited to porous silica but should be readily applied to immobilization of DNA to glass surfaces for fluorescence imaging of hybridization and DNA microarrays. The application of this chemistry to DNA immobilization on porous silica produces locally high DNA concentrations on the interior of the particles that allow *in situ* investigations of the structure and reactivity of immobilized DNA by confocal Raman microscopy. The combination of stable DNA immobilization on high-surface area porous supports with a label-free vibrational spectroscopy paves the way for relating DNA structure to its functionality with respect to interactions with either small molecules or proteins. Confocal Raman microscopy was also found to be a powerful method for monitoring the reaction steps in generating the stable binding of DNA to a silica surface. This method could be used for following the interfacial chemistry of other conjugation chemistries to immobilize biological molecules to silica or glass surfaces.

ASSOCIATED CONTENT

Supporting Information.

Additional information on the reaction scheme to immobilize thiol-functionalized DNA to thiolated silica, ESI-TOF-MS analysis of the thiol-DNA bismaleimide coupling products, quantification of surface-immobilized DNA, Raman spectroscopy of the hydrolysis of a phenyl-thiosuccinimide, comparison of the stability of alkyl-bismaleimide coupling, and an SEM image of the porous silica used as the support for DNA immobilization.

ACKNOWLEDGEMENTS

This work was supported by the National Science Foundation under Grant CHE-1904424. The authors are grateful to W. Mike Hanson of the University of Utah Core DNA Synthesis Facility and to Hsiao-Nung Chen and Jim Muller of the Department of Chemistry Mass Spectrometry Lab for contributions to this project. The authors also acknowledge informative conversations with Andrew Roberts on bioconjugation chemistry.

REFERENCES

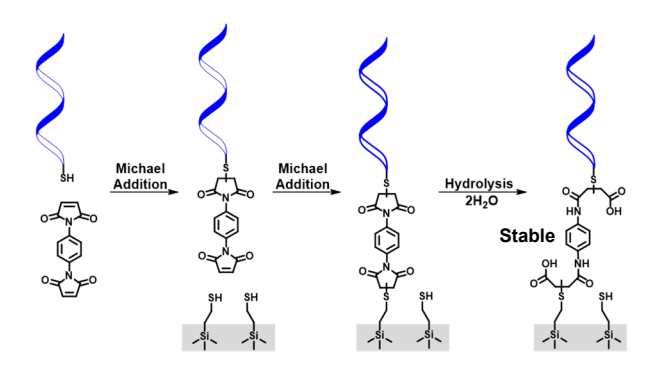
- (1) Li, H.; Somerson, J.; Xia, F.; Plaxco, K.W. Electrochemical DNA-Based Sensors for Molecular Quality Control: Continuous, Real-Time Melamine Detection in Flowing Whole Milk. *Anal. Chem.* **2018**, *90*, 10641-10645.
- (2) Arroyo-Currás, N.; Ortega, G.; Copp, D.A.; Ploense, K.L.; Plaxco, Z.A.; Kippin, T.E.; Hespanha, J.P.; Plaxco, K.W. High-Precision Control of Plasma Drug Levels Using Feedback-Controlled Dosing. *ACS Pharmacol. Transl. Sci.* **2018**, *1*, 110-118.
- (3) Baker, B.R.; Lai, R.Y.; Wood, M.S.; Doctor, E.H.; Heeger, A.J.; Plaxco, K.W. An Electronic, Aptamer-Based Small-Molecule Sensor for the Rapid, Label-Free Detection of Cocaine in Adulterated Samples and Biological Fluids. *J. Am. Chem. Soc.* **2006**, *128*, 3138-3139.
- (4) Xiao, Y.; Qu, X.; Plaxco, K.W.; Heeger, A.J. Label-Free Electrochemical Detection of DNA in Blood Serum via Target-Induced Resolution of an Electrode-Bound DNA Pseudoknot. *J. Am. Chem. Soc.* **2007**, *129*, 11896-11897.
- (5) DeRisi, J.; Penland, L.; Brown, P.; Bittner, M.L.; Meltzer, P.S.; Ray, M.; Chen, Y.; Su, Y.A.; Trent, J.M. Use of a cDNA microarray to analyse gene expression patterns in human cancer. *Nature Genetics* **1996**, *14*, 457-460.
- (6) Kononen, J.; Bubendorf, L.; Kallionimeni, A.; Bärlund, M.; Schraml, P.; Leighton, S.; Torhorst, J.; Mihatsch, M.J.; Sauter, G.; Kallionimeni, O.-P. Tissue microarrays for high-throughput molecular profiling of tumor specimens. *Nature Medicine* **1998**, *4*, 844-847.
- (7) Alizadeh, A.A.; Eisen, M.B.; Davis, R.E.; Ma, C.; Lossos, I.S.; Rosenwald, A.; Boldrick, J.C.; Sabet, H.; Tran, T.; Yu, X.; Powell, J.I.; Yang, L.; Marti, G.E.; Moore, T.; Hudson, J.; Lu, L.; Lewis, D.B.; Tibshirani, R.; Sherlock, G.; Chan, W.C.; Greiner, T.C.; Weisenburger, D.D.; Armitage, J.O.; Warnke, R.; Levy, R.; Wilson, W.; Grever, M.R.; Byrd, J.C.; Botstein, D.; Brown, P.O.; Staudt, L.M. Distinct types of diffuse large B-cell lymphoma identified by gene expression profiling. *Nature* **2000**, *403*, 503-511.
- (8) Miao, Y.; Cui, T.; Leng, F.; Wilson, W.D. Inhibition of high-mobility-group A2 protein binding to DNA by netropsin: A biosensor-surface plasmon resonance assay. *Anal. Biochem.* **2008**, *374*, 7-15.
- (9) Liu, Y.; Kumar, A.; Depauw, S.; Nhili, R.; David-Cordonnier, M.-H.; Lee, M.P.; Ismail, M.A.; Farahat, A.A.; Say, M.; Chackal-Catoen, S.; Batista-Parra, A.; Neidle, S.; Boykin, D.W.; Wilson, W.D. Water-Mediated Binding of Agents that Target the DNA Minor Groove. *J. Am. Chem. Soc.* **2011**, *133*, 10171-10183.

- (10) Doughty, B.; Rao, Y.; Kazer, S.W.; Kwok, S.J.J.; Turro, N.J.; Eisenthal, K.B. Binding of the Anti-Cancer Drug Daunomycin to DNA Probed by Second Harmonic Generation. *J. Phys. Chem. B* **2013**, *117*, 15285-15289.
- (11) Iida, K.; Nakamura, T.; Yoshida, W.; Tera, M.; Nakabayashi, K.; Hata, K.; Ikebukuro, K.; Nagasawa, K. Fluorescent-Ligand-Mediated Screening of G-Quadruplex Structures Using a DNA Microarray. *Angew. Chem. Int. Ed.* **2013**, *52*, 12052-12055.
- (12) Morris, F.D.; Peterson, E.M.; Heemstra, J.M.; Harris, J.M. Single-Molecule Kinetic Investigation of Cocaine-Dependent Split-Aptamer Assembly. *Anal. Chem.* **2018**, *90*, 12964-12970.
- (13) Ray, S.; Tillo, D.; Boer, R.E.; Assad, N.; Barshai, M.; Wu, G.; Orenstein, Y.; Yang, D.; Schneekloth, J.S.; Vinson, C. Custom DNA Microarrays Reveal Diverse Binding Preferences of Proteins and Small Molecules to Thousands of G-Quadruplexes. *ACS Chem. Biol.* **2020**, *15*, 925-935.
- (14) Lackey, H.H.; Peterson, E.M.; Harris, J.M.; Heemstra, J.M. Probing the Mechanism of Structure-Switching Aptamer Assembly by Super-Resolution Localization of Individual DNA Molecules. *Anal. Chem.* **2020**, *92*, 6909-6917.
- (15) Bulyk, M.L.; Huang, X.; Choo, Y.; Church, G.M. Exploring the DNA-binding specificities of zinc fingers with DNA microarrays. *Proc. Natl. Acad. Sci. U. S. A.* **2001**, *98*, 7158-7163.
- (16) Mukherjee, S.; Berger, M.F.; Jona, G.; Wang, X.S.; Muzzey, D.; Snyder, M.; Young, R.A.; Bulyk, M.L. Rapid analysis of the DNA-binding specificities of transcription factors with DNA microarrays. *Nature Genetics* **2004**, *36*, 1331-1339.
- (17) Berger, M.F.; Philippakis, A.A.; Qureshi, A.M.; He, F.S.; Estep, P.W.; Bulyk, M.L. Compact, universal DNA microarrays to comprehensively determine transcription-factor binding site specificities. *Nat. Biotechnol.* **2006**, *24*, 1429-1435.
- (18) Peterson, E.M.; Manhart, M.W.; Harris, J.M. Single-Molecule Fluorescence Imaging of Interfacial DNA Hybridization Kinetics at Selective Capture Surfaces. *Anal. Chem.* **2016**, *88*, 1345-1354.
- (19) Peterson, E.M.; Harris, J.M. Identification of Individual Immobilized DNA Molecules by Their Hybridization Kinetics Using Single-Molecule Fluorescence Imaging. *Anal. Chem.* **2018**, *90*, 5007-5014.
- (20) Peterson, E.M.; Reece, E.J.; Li, W.; Harris, J.M. Super-Resolution Imaging of Competitive Unlabeled DNA Hybridization Reveals the Influence of Fluorescent Labels on Duplex Formation and Dissociation Kinetics. *J. Phys. Chem. B* **2019**, *123*, 10746-10756.

- (21) Saito, F.; Noda, H.; Bode, J.W. Critical Evaluation and Rate Constants of Chemoselective Ligation Reactions for Stoichiometric Conjugations in Water. *ACS Chem. Biol.* **2015**, *10*, 1026-1033.
- (22) Ravasco, J.M.J.M.; Faustino, H.; Trindade, A.; Gois, P.M.P. Bioconjugation with Maleimides: A Useful Tool for Chemical Biology. *Chemistry A European Journal* **2019**, *25*, 43-59.
- (23) Kolb, H.C.; Finn, M.G.; Sharpless, K.B. Click Chemistry: Diverse Chemical Function from a Few Good Reactions. *Angew. Chem. Int. Ed.* **2001**, *40*, 2004-2021.
- (24) Pounder, R.J.; Stanford, M.J.; Brooks, P.; Richards, S.P.; Dove, A.P. Metal free thiol—maleimide 'Click' reaction as a mild functionalisation strategy for degradable polymers. *Chem. Commun.* **2008**, 5158-5160.
- (25) Szijj, P.A.; Bahou, C.; Chudasama, V. Minireview: Addressing the retro-Michael instability of maleimide bioconjugates. *Drug Discovery Today: Technologies* **2018**, *30*, 27-34.
- (26) Fontaine, S.D.; Reid, R.; Robinson, L.; Ashley, G.W.; Santi, D.V. Long-Term Stabilization of Maleimide–Thiol Conjugates. *Bioconjugate Chem.* **2015**, *26*, 145-152.
- (27) Wu, H.; Levalley, P.J.; Luo, T.; Kloxin, A.M.; Kiick, K.L. Manipulation of Glutathione-Mediated Degradation of Thiol–Maleimide Conjugates. *Bioconjugate Chem.* **2018**, *29*, 3595-3605.
- (28) Machida, M.; Machida, M.I.; Kanaoka, Y. Hydrolysis of N-substituted maleimides: Stability of fluorescence thiol reagents in aqueous media. *Chem. Pharm. Bull.* **1977**, *25*, 2739-2743.
- (29) Knight, P. Hydrolysis of p-NN'-phenylenebismaleimide and its adducts with cysteine. Implications for cross-linking of proteins. *Biochem. J* **1979**, *179*, 191-197.
- (30) Baldwin, A.D.; Kiick, K.L. Tunable Degradation of Maleimide–Thiol Adducts in Reducing Environments. *Bioconjugate Chem.* **2011**, *22*, 1946-1953.
- (31) Sun, P.; Scharnweber, T.; Wadhwani, P.; Rabe, K.S.; Niemeyer, C.M. DNA-Directed Assembly of a Cell-Responsive Biohybrid Interface for Cargo Release. *Small Methods* **2021**, *5*, 2001049.
- (32) Myres, G.J.; Peterson, E.M.; Harris, J.M. Confocal Raman Microscopy Enables Label-Free, Quantitative, and Structurally Informative Detection of DNA Hybridization at Porous Silica Surfaces. *Anal. Chem.* **2021**, *93*, 7978-7986.
- (33) Christie, R.J.; Fleming, R.; Bezabeh, B.; Woods, R.; Mao, S.; Harper, J.; Joseph, A.; Wang, Q.; Xu, Z.-Q.; Wu, H.; Gao, C.; Dimasi, N. Stabilization of cysteine-linked antibody drug conjugates with N-aryl maleimides. *J. Controlled Release* **2015**, *220*, 660-670.

- (34) Kitagawa, T.; Shimozono, T.; Aikawa, T.; Yoshida, T.; Nishimura, H. Preparation and characterization of hetero-bifunctional cross-linking reagents for protein modifications. *Chem. Pharm. Bull.* **1981**, *29*, 1130-1135.
- (35) Kitt, J.P.; Harris, J.M. Confocal Raman Microscopy for in Situ Detection of Solid-Phase Extraction of Pyrene into Single C18–Silica Particles. *Anal. Chem.* **2014**, *86*, 1719-1725.
- (36) Brandt, N.N.; Brovko, O.O.; Chikishev, A.Y.; Paraschuk, O.D. Optimization of the Rolling-Circle Filter for Raman Background Subtraction. *Appl. Spectrosc.* **2006**, *60*, 288-293.
- (37) Kim, D.; Zuidema, J.M.; Kang, J.; Pan, Y.; Wu, L.; Warther, D.; Arkles, B.; Sailor, M.J. Facile Surface Modification of Hydroxylated Silicon Nanostructures Using Heterocyclic Silanes. *J. Am. Chem. Soc.* **2016**, *138*, 15106-15109.
- (38) Mondin, G.; Lohe, M.R.; Wisser, F.M.; Grothe, J.; Mohamed-Noriega, N.; Leifert, A.; Dörfler, S.; Bachmatiuk, A.; Rümmeli, M.H.; Kaskel, S. Electroless copper deposition on (3-mercaptopropyl)triethoxysilane-coated silica and alumina nanoparticles. *Electrochim. Acta* **2013**, *114*, 521-526.
- (39) Gasser-Ramirez, J.L.; Harris, J.M. Confocal Raman Microscopy of the Interfacial Regions of Liquid Chromatographic Stationary-Phase Materials. *Anal. Chem.* **2009**, *81*, 2869-2876.
- (40) Sinden, R.R. DNA Structure and Function; Academic Press: San Diego, 1994.
- (41) Lyon, R.P.; Setter, J.R.; Bovee, T.D.; Doronina, S.O.; Hunter, J.H.; Anderson, M.E.; Balasubramanian, C.L.; Duniho, S.M.; Leiske, C.I.; Li, F.; Senter, P.D. Self-hydrolyzing maleimides improve the stability and pharmacological properties of antibody-drug conjugates. *Nat. Biotechnol.* **2014**, *32*, 1059-1062.
- (42) Tyagi, S.; Kramer, F.R. Molecular Beacons: Probes that Fluoresce upon Hybridization. *Nat. Biotechnol.* **1996**, *14*, 303-308.
- (43) Tan, W.; Wang, K.; Drake, T.J. Molecular beacons. *Curr. Opin. Chem. Biol.* **2004**, *8*, 547-553.
- (44) Watkins, H.M.; Vallée-Bélisle, A.; Ricci, F.; Makarov, D.E.; Plaxco, K.W. Entropic and Electrostatic Effects on the Folding Free Energy of a Surface-Attached Biomolecule: An Experimental and Theoretical Study. *J. Am. Chem. Soc.* **2012**, *134*, 2120-2126.
- (45) Watkins, H.M.; Simon, A.J.; Ricci, F.; Plaxco, K.W. Effects of Crowding on the Stability of a Surface-Tethered Biopolymer: An Experimental Study of Folding in a Highly Crowded Regime. *J. Am. Chem. Soc.* **2014**, *136*, 8923-8927.

- (46) Benevides, J.M.; Thomas, G.J. Characterization of DNA structures by Raman spectroscopy: high-salt and low-salt forms of double helical poly(dG-dC) in H2O and D2O solutions and application to B, Z and A-DNA. *Nucleic Acids Res.* **1983**, *11*, 5747-5761.
- (47) Duguid, J.G.; Bloomfield, V.A.; Benevides, J.M.; Thomas, G.J., Jr. DNA melting investigated by differential scanning calorimetry and Raman spectroscopy. *Biophys. J.* **1996**, *71*, 3350-3360.
- (48) Movileanu, L.; Benevides, J.M.; Thomas, G.J. Temperature dependence of the raman spectrum of DNA. II. Raman signatures of premelting and melting transitions of poly(dA)·poly(dT) and comparison with poly(dA-dT)·poly(dA-dT). *Biopolymers* **2002**, *63*, 181-194.
- (49) Schellman, J.A.; Stigter, D. Electrical double layer, zeta potential, and electrophoretic charge of double-stranded DNA. *Biopolymers* **1977**, *16*, 1415-1434.
- (50) Dupuis, Nicholas F.; Holmstrom, Erik D.; Nesbitt, David J. Single-Molecule Kinetics Reveal Cation-Promoted DNA Duplex Formation Through Ordering of Single-Stranded Helices. *Biophys. J.* **2013**, *105*, 756-766.
- (51) Okahata, Y.; Kawase, M.; Niikura, K.; Ohtake, F.; Furusawa, H.; Ebara, Y. Kinetic Measurements of DNA Hybridization on an Oligonucleotide-Immobilized 27-MHz Quartz Crystal Microbalance. *Anal. Chem.* **1998**, *70*, 1288-1296.
- (52) Benevides, J.M.; Overman, S.A.; Thomas, G.J. Raman, polarized Raman and ultraviolet resonance Raman spectroscopy of nucleic acids and their complexes. *J. Raman Spectrosc.* **2005**, *36*, 279-299.
- (53) Iler, R.K. *The Chemistry of Silica: Solubility, Polymerization, Colloid and Surface Properties, and Biochemistry*; Wiley: New York, 1979.
- (54) Hill, H.D.; Millstone, J.E.; Banholzer, M.J.; Mirkin, C.A. The Role Radius of Curvature Plays in Thiolated Oligonucleotide Loading on Gold Nanoparticles. *ACS Nano* **2009**, *3*, 418-424.
- (55) Cederquist, K.B.; Keating, C.D. Curvature Effects in DNA:Au Nanoparticle Conjugates. *ACS Nano* **2009**, *3*, 256-260.



TOC GRAPHIC